Arabian Journal of Chemistry (2015) **8**, 105–117

King Saud University

Arabian Journal of Chemistry

www.ksu.edu.sa
www.sciencedirect.com

ORIGINAL ARTICLE

Removal of toxic chromium from aqueous solution, wastewater and saline water by marine red alga *Pterocladia capillacea* and its activated carbon

Ahmed El Nemr *, **AmanyEl-Sikaily, Azza Khaled, Ola Abdelwahab**

Department of Pollution, Environmental Division, National Institute of Oceanography and Fisheries, El Anfoushy, Kayet Bey, Alexandria, Egypt

Received 17 October 2010; accepted 16 January 2011
Available online 21 January 2011

KEYWORDS

Marine algae;
Pterocladia capillacea;
Biosorption;
Chromium;
Wastewater;
Saline water;
Isotherm models

Abstract *Pterocladia capillacea*, a red marine macroalgae, was tested for its ability to remove toxic hexavalent chromium from aqueous solution. A new activated carbon obtained from *P. capillacea* via acid dehydration was also investigated as an adsorbent for toxic chromium. The experiments were conducted to study the effect of important parameters such as pH, chromium concentration and adsorbent weight. Batch equilibrium tests at different pH conditions showed that at pH 1.0, a maximum chromium uptake was observed for both inactivated dried red alga *P. capillacea* and its activated carbon. The maximum sorption capacities for dried red alga and its activated carbon were about 12 and 66 mg g^{-1}, respectively, as calculated by Langmuir model. The ability of inactivated red alga *P. capillacea* and developed activated carbon to remove chromium from synthetic sea water, natural sea water and wastewater was investigated as well. Different isotherm models were used to analyze the experimental data and the models parameters were evaluated. This study showed that the activated carbon developed from red alga *P. capillacea* is a promising activated carbon for removal of toxic chromium.

1. Introduction

Heavy metal pollution represents an important environmental problem due to toxic effects and accumulation throughout the food chain. These pollutants are toxic and non-biodegradable and probably have health effect (Pellerin and Booker, 2000). Several industries like paint and pigment manufacturing, stainless steel production, corrosion control, textile, leather tanning, chrome electroplating, metal finishing industries, wood preservation, photography, etc. discharge effluent containing hexavalent chromium, Cr^{6+}, to surface water. Hexavalent chromium is toxic and a suspected carcinogen material and it is quite soluble in the aqueous phase almost over the entire pH range and mobile in the natural environment (Gode and Pehlivan, 2005). A very high positive redox potential is demonstrated for acidic solution of hexava-

* Corresponding author. Tel./fax: +20 35740944.
E-mail address: ahmedmoustafaelnemr@yahoo.com (A. El Nemr).
Peer review under responsibility of King Saud University.

ELSEVIER Production and hosting by Elsevier

http://dx.doi.org/10.1016/j.arabjc.2011.01.016
1878-5352

lent chromium which is strongly oxidizing and unstable in the presence of electron donors. Several species can be obtained from hexavalent chromium depending on pH and its total concentration. The $HCrO_4^{2-}$ form exists in the solution if the solution pH > 7, while in the pH between 1 and 6, CrO_4^{2-} is predominant. Therefore, within the normal pH range in natural waters, the CrO_4^{2-}, CrO_4^{2-} and $Cr_2O_7^{2-}$ ions are forms expected and they constituted a lot of hexavalent chromium compounds, which are quite soluble and mobile in water streams (Gode and Pehlivan, 2005; Ko et al., 2002). The maximum permissible levels for Cr^{3+} and Cr^{6+} ions in wastewater are 5 and 0.05 mg L^{-1}, respectively. They exist as low levels in the environment. While Cr^{3+} apparently plays an essential role in plant and animal metabolism, the Cr^{6+} is directly toxic to bacteria, plants and animals (Richard and Bourg, 1991). The most severe chromium compounds are chromium oxide and chromium sulfate as trivalent and chromium trioxide, chromic acid and dichromates as hexavalent chromium (Ramos et al., 1994).

Sorption process has been extensively used to remove toxic metals from aquatic medium using low cost adsorbents such as agriculture wastes and activated carbon developed from agriculture wastes (Babel and Kurniawan, 2003; Demirbas et al., 2004; Ahalya et al., 2005; El Nemr et al., 2006, 2007, 2010; Abdelwahab et al., 2007; Wang et al., 2009). Among the most promising biomaterials studied is algal biomass (Vijayaraghavan et al., 2005; Kalyani et al., 2004; Gupta et al., 2001; Zeroual et al., 2003; Abdelwahab et al., 2006a,b; El-Sikaily et al., 2006; Han et al., 2008; Gupta and Rastogi, 2009; Ncibi et al., 2009; Deng et al., 2009; Zakhama et al., 2011). The presence of carboxylic (–COOH), sulfonic (–SO_3H) and hydroxyl (–OH) groups in the marine algae polysaccharides are believed to be responsible for impressive metal uptake by marine algae (McKay et al., 1999; Davis et al., 2003). Moreover, the macroscopic structures for marine algae present a convenient basis for the production of biosorbent particles suitable for sorption process applications (Vieira and Volesky, 2000).

As the most toxic species of chromium cannot be removed directly by precipitation, the main objective of this study was to evaluate the possibility of using dried red alga *Pterocladia capillacea* (DRA) and activated carbon developed from *P. capillacea* (CRA) as sorbents for the elimination of Cr^{6+} from polluted waters by systematic evaluation of the parameters involved, such as pH, sorbents mass, initial chromium concentration and time. The interference of the real wastewater and saline water on the Cr^{6+} sorption was additionally investigated.

2. Materials and methods

2.1. Biomass

Fresh red algal biomass of *P. capillacea* species was collected from Abo-Quir Bay, Alexandria, Egypt. Before being dried, it was washed with sea water and then with tap water followed by washing with distilled water. After this, the clean algal biomass was sun dried for two days followed by air oven drying at 105 °C for 72 h, and the dried red alga (DRA) was milled and sieved to select particles ⩽0.063 mm for use (Deng et al., 2009; Gupta and Rastogi, 2009).

2.2. Activated carbon from red alga (CRA)

The dried red algal (DRA) biomass of *P. capillacea* (1.0 kg) was added in small portion to 600 ml of 98% H_2SO_4 and the resulting reaction mixture was kept for 1 h at room temperature followed by refluxing for 5 h in an efficient fume hood. After cooling to room temperature, the reaction mixture was poured onto cold water (4 L) and filtered. The resulting material was washed repeatedly with water and then soaked in 1% $NaHCO_3$ solution to remove any remaining acid. The obtained carbon was then washed with distilled water until pH of the activated carbon reached 6, dried in an oven at 250 °C for 1 h in the absence of oxygen and sieved to the particle size ⩽0.063 mm and kept in a glass bottle until used.

2.3. Preparation of synthetic solution

A stock solution of 1.0 g L^{-1} was prepared by dissolving the 2.831 g of potassium dichromate ($K_2Cr_2O_7$) in 100 ml and completed to 1000 ml with distilled water. Concentrations ranged between 5 and 100 mg L^{-1} were prepared from the stock solution to have the standard curve. All the chemicals used throughout this study were of analytical-grade reagents. Double-distilled water was used for preparing all of the solutions and reagents. The initial pH is adjusted with 0.1 M HCl or 0.1 M NaOH. All the sorption experiments were carried out at room temperature (25 ± 2 °C).

The concentration of Cr^{6+} ions in solution was measured by using an indirect UV–visible spectrophotometric method based on the reaction of Cr^{6+} and 1,5-diphenylcarbazide, which forms a red-violet colored complex (Gilcreas et al., 1965). The absorbance of the colored complex was measured using UV–VIS spectrophotometer (Milton Roy, Spectronic 21D) using silica cells of path length 1 cm at wavelength λ 540 nm, and Cr^{6+} concentration was determined by comparing absorbance to a calibration curve mentioned above. All the experiments are duplicated and only the mean values are reported. The maximum deviation observed was less than ±5% (Ncibi et al., 2009).

2.4. Red alga characterization

The functional groups present in the red alga and its activated carbon were characterized by a Fourier transform infrared (FT-IR), using KBr disks to prepare the alga samples.

The X-ray diffraction spectrum was obtained by passing the sample through 44 μ copper target. Samples were exposed to X-ray (λ = 1.5418 Å) with the 2θ angle, scan range varying between 4°–9° and scan speed 2 deg/min. The applied voltage and current were 30 kV and 30 mA, respectively.

The morphological characteristics of red alga and its activated carbon were evaluated by using a JEOL JSM-6360 scanning electron microscope with an electron acceleration voltage of 20 kV.

2.5. Simulation studies

Synthetic sea water was prepared by dissolving 35 g of NaCl in 1000 ml distilled water and used instead of distilled water. Different weights of chromium were dissolved in the synthetic sea water to obtain different concentrations of Cr^{6+}.

Natural sea water was collected from Eastern Harbor, Alexandria, Egypt and filtered using Whatman filter paper. The clear natural seawater was used instead of distilled water used above to prepare different concentrations of Cr^{6+}.

Wastewater was collected from El-Emoum drain (contains several industrial effluents and agriculture drain from Alexandria Governorate) near lake Maruit, Alexandria, Egypt. The collected wastewater was filtered through Whatman filter paper to remove suspended particulates and used as above for preparing of different concentrations of Cr^{6+}.

2.6. Batch biosorption studies

2.6.1. Effect of pH on chromium biosorption

The effect of pH on the equilibrium uptake of chromium ions was investigated by employing different initial concentrations of Cr^{+6} (75 mg L^{-1}) and 5 g L^{-1} of DRA and CRA. The initial pH values were adjusted to 1, 2, 3, 4, 5, 6 and 7 with 0.1 M HCl or 0.1 M NaOH. The suspensions were shaken at room temperature (25 ± 2 °C) using agitation speed (200 rpm) for the minimum contact time required to reach the equilibrium (120 min) and the amount of chromium adsorbed determined (Malkoç and Nuhoglu, 2003; Wang et al., 2009).

2.6.2. Effect of sorbents dose

The effect of sorbents dose on the equilibrium uptake of chromium ions was investigated with sorbent concentrations of 3, 4, 5 and 10 g L^{-1}. The experiments were performed by shaking known chromium concentration with the above different sorbent concentrations to the equilibrium uptake (120 min) and the amount of chromium adsorbed determined (Wang et al., 2009).

2.6.3. Kinetics studies

Sorption studies were conducted in 300 ml conical flasks at solution pH 1.0. DRA biomass (10 g L^{-1}) or CRA (3, 4 and 5 g L^{-1}) was thoroughly mixed individually with 100 ml of chromium solution (5, 10, 20, 30, 50, 75, 100 and 125 mg L^{-1}) and the suspensions were shaken at room temperature (27 °C). Samples of 0.5 ml were collected from the duplicate flasks at required time intervals viz. 5, 10, 20, 30, 45, 60, 90 and 120 min and were centrifuged for 5 min. The clear solutions were analyzed for residual chromium concentration in the solution (Zakhama et al., 2011).

2.6.4. Sorption isotherm

Batch sorption experiments were carried out in 300 ml conical flasks at 27 °C on a shaker for 120 min. The DRA (1.0 g) and CRA (0.3, 0.4 and 0.5 g) were thoroughly mixed with 100 ml of chromium solutions. The isotherm studies were performed by varying the initial chromium concentrations from 5 to 125 mg L^{-1} at pH 1.0. The pH value was adjusted using 0.1 M HCl or 0.1 M NaOH before addition of biomass and was maintained throughout the experiment. After shaking the flasks for 120 min, the reaction mixture was analyzed for the residual chromium concentration (Zakhama et al., 2011).

Sorption of Cr^{+6} from its solutions in synthetic sea water, natural sea water and wastewater was studied using 5 g L^{-1} of red alga and its activated carbon and Cr^{6+} concentrations 125 mg L^{-1} and initial pH 1.0.

3. Results and discussion

3.1. Fourier transform infrared spectroscopy (FT-IR) analysis

The FT-IR technique is an important tool to identify some characteristic functional groups, which are capable of adsorbing metal ions. The FT-IR spectra for red alga *P. capillacea* and its activated carbon are shown in Fig. 1a and b and Table 1. The FT-IR spectra display number of absorption peaks, the bands at 3433 and 3436 cm^{-1} in both charts of red alga and its activated carbon representing bonded –OH group on their surface (Kamath and Proctor, 1998). Aliphatic C–H group is represented by the peak at 2925 cm^{-1}. The peaks located at 1637 and 1635 cm^{-1} are characteristics for C═O stretching for aldehydes and ketones, which can be conjugated or non-conjugated to aromatic rings (Cesar Ricardo and Marco Aurelio, 2004), while deformations related to C–H and C–O bonds were observed in carbon of red alga at 1062 cm^{-1} this may be due to carbonization method. Also, a peak observed at 1182 cm^{-1} in chart of red alga carbon indicates the presences of bisulfate (HSO_4^-). The peaks at 873, (594–584 cm^{-1}), 445 and 381 cm^{-1} are due to the presences of H_2PO^{4-}, PO_4^{2-} and metal oxide. These different functional groups have a high affinity toward heavy metals so that they can form complex with metal ions (Hawari and Mulligan, 2006). Untreated biomass generally contains light metal ions such as K^+, Na^+ Ca^{2+} and Mg^{2+} (Padilha et al., 2005; Malkoc and Nuhoglu, 2006). The biosorption process of nickel, copper and cadmium can be mainly accounted for by ion exchange with calcium (Hawari and Mulligan, 2006). There was a significant release of Ca^{2+}, Mg^{2+}, K^+ and H^+ from the biosorbent due to uptake of Cu (II), Cr (III, VI) and Ni (II). This might indicate the displacement of these cations by the metals (Villaescusa et al., 2004).

3.2. X-ray diffraction analysis

The X-ray diffraction patterns for red alga and its activated carbon are shown in Fig. 2. The humb peak which appears in the front of sheet of X-ray diffraction of *P. capillacea* reflects the presence of high percent of organic compounds. The middle zone of the X-ray sheet is occupied by significant peaks ranged from 2θ = 11.95–24.178 with highest value recorded at 22.68 corresponding to d-spacing values 7.39, 3.67 and 3.91 Å, which proves the presence of silicate as orthoclase. This finding is in agreement with the FT-IR which reveals the presence of silicate group. The carbonization of alga with sulfuric acid affects on the crystal form structure of the alga. The humb which appeared in the red alga disappeared in its activated carbon. In addition, the mean peak in the red alga at 2θ = 77.45 also disappeared which indicates that the treatment arranged the crystal lattice of the samples. In the carbon of alga the main peak recorded at 2θ = 25.8 is corresponding to the presence of silicate in quartz form (Griffen, 1971).

3.3. Scanning electron microscope (SEM)

Scanning electron microscope of red alga and its activated carbon is shown in Fig. 3. The morphology of this material can facilitate the sorption of metals, due to the irregular surface of the alga, thus makes the sorption of metal possible on

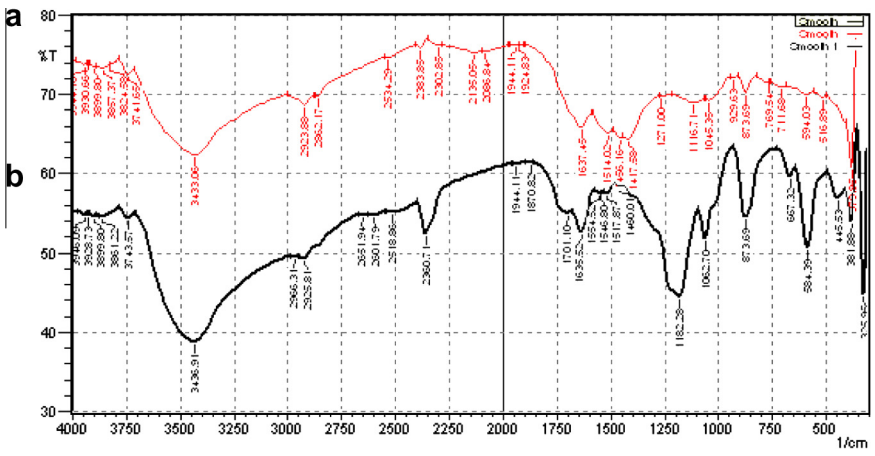

Figure 1 (a) The FT-IR spectra of red alga *P. capillacea* biomass before sorption and (b) the FT-IR spectra of carbon red alga *P. capillacea* biomass before sorption.

Table 1 The FT-IR spectral characteristics of red alga (*P. capillacea*) and its carbon.

IR peak	Frequency (cm^{-1})		Assignment
	Red alga	Carbon red alga	
1	3433.05	3436.91	Bonded –OH group
2	2922.00	2925.81	Aliphatic C–H group
3	2383.85	2360.71	Dibasic phosphate (HPO_4^{2-})
4	1637.45	1635.50	C═O stretching
5	–	1182.20	Bisulfate (HSO_4^-)
6	–	1062.70	C–H and C–O deformation
7	873.69	873.070	Silicate
8	594.03	584.39	$H_2PO_4^-$ or PO_4^{2-}
9	–	445.53	Metal compounds
10	–	381.88	Metal oxide

different parts of this material. So, based on the morphology, as well as on the fact that high amounts of silicate which concentrated on the alga and its carbon, it can be concluded that this material presents an adequate morphological profile to adsorb metal ions.

3.4. Effect of pH on Cr^{6+} uptake

The Fig. 4 shows that the lowest sorption occurred at pH 7.0 and the greatest sorption occurred at pH 1.0. Hence all sorption experiments were conducted at the acidic pH (pH 1.0) (Malkoç and Nuhoglu, 2003, 2006). The pH dependence of metal sorption can largely be related to the type and ionic state of these functional groups and also on the metal chemistry in solution. Moreover, at very low pH values (acidic), the surface of sorbent would also be surrounded by the hydronium ions which enhance the Cr^{6+} interaction with binding sites of DRA and CRA by greater attractive forces. Sorption of Cr^{6+} below pH 3 suggests that negatively charged species (chromate/dichromate in the sample solution) bind through electrostatic attraction to positively charged functional groups on the surface of algae because at this pH more functional group carrying positive charge would be exposed. At pH above 3, the algae possess more functional groups carrying a net negative charge, which tends to repulse the anions. However, there is also Cr^{6+} ions removal occurred above pH 3, as indicated by Fig. 4, but the rate of removal is considerably reduced. Therefore, the mechanism of the sorption occurs basically due to the interaction of negatively charged species of Cr and the positive charged occurred on the adsorbent surface, which may be proved by decreasing of the sorption capacity by decreasing the acidity of the solution Fig. 5.

3.5. Effect of adsorbent dose on metal sorption

The effects of DRA and CRA dosage on the removal of Cr^{6+} from its aqueous solutions were investigated using different

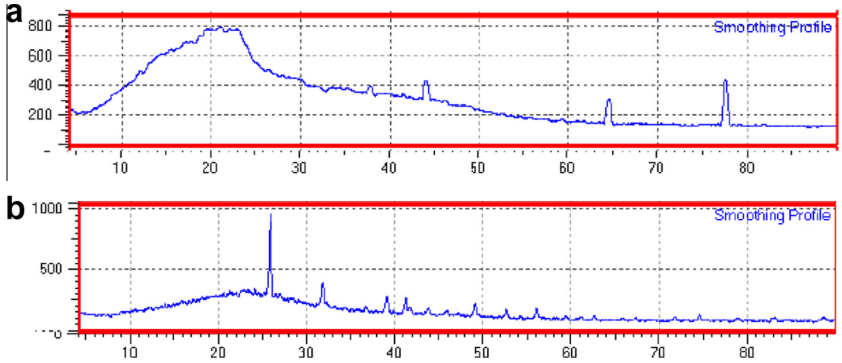

Figure 2 X-ray diffractograms of (a) red alga *P. capillacea* and (b) carbon red alga *P. capillacea*.

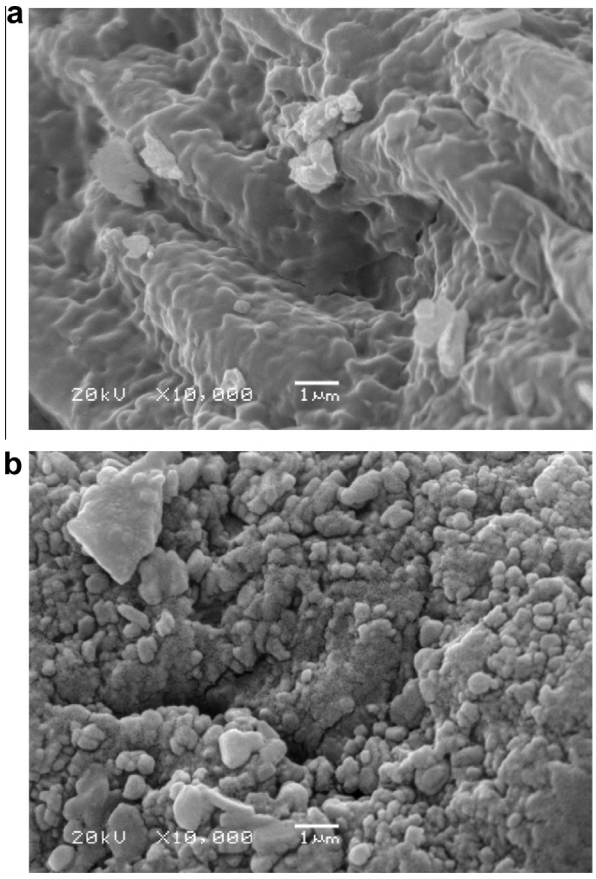

Figure 3 Scanning electron micrograph of (a) red alga *P. capillacea* and (b) carbon of red alga *P. capillacea*.

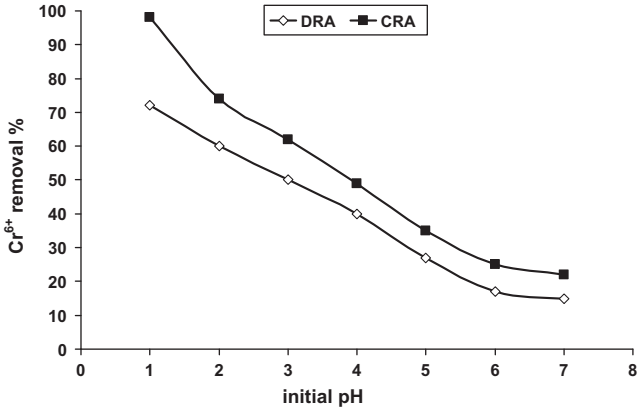

Figure 4 Effect of initial pH on sorption of Cr^{6+} onto DRA and CRA.

adsorbent concentrations. DRA and CRA dosage were varied from 1 to 10 g L^{-1} and their effect on the sorption capacities of Cr^{6+} ion were studied at pH of 1 and 125 mg L^{-1} initial chromium concentration. Fig. 6 shows increase in biomass dose after optimum value did not show corresponding increase in the Cr^{6+} ion uptake from the solution. Interaction of sorbent and metal ions is generally electrostatic in nature on the binding sites present on the surface of sorbent. For a given constant of sorbent concentration, the initial Cr^{6+} ion sorption increased up to the stage of saturation of all the binding sites and further increase in the dose of sorbent did not change the metal sorption/biomass ratio. Also, the high concentration of sorbent resulted in screen effect of dense outer layer of cells and blocking the binding site from metal ions, resulting in lower metal removal per unit of sorbent (Meena et al., 2004).

3.6. Effect of contact time and initial Cr^{6+} ion concentration

The results of percentage removal of Cr^{6+} at pH 1 with increasing of contact time using DRA and CRA are presented in Fig. 6, respectively. The maximum amount of Cr^{6+} uptake was observed after 60 min. Increase in contact time from 60 to 180 min did not result in corresponding increase in sorption. It is a rapid process as most of the sorption (80–85%) was completed in the initial 45 min. These results indicated that the sorption sites were bind up in the initial 60 min by the metal ions passively. After this, the increase in contact time might not help for more sorption of metal ions with this sorbent (Meena et al., 2004). The uptake of metal ions was observed for different initial ion concentration of Cr^{6+} at optimum contact time and sorbent dose. The results revealed that an increase in metal ion concentration resulted in gradual decrease in percent sorption of Cr^{6+} up to 100 mg L^{-1} and after that a sharp decrease in metal uptake percentage. An increase in initial concentration of metal ions resulted in the lowering of metal ion uptake due to reduction in ratio of sorptive surface to ion concentration (Chandra et al., 2005; Meena et al., 2004).

3.7. Isotherm data analysis

In order to model the sorption behavior and calculate the sorption capacity of DRA and CRA, sorption isotherms were studied. The most widely accepted surface sorption models for single-solute systems are the Langmuir and Freundlich models. The correlation with the amount of adsorbent and the liquid-phase concentration was tested with the Langmuir, Freundlich, Temkin and Dubinin–Radushkevich (D–R) isotherm equations. Linear regression is frequently used to determine the best-fitting isotherm, and the method of least squares has been used for finding the parameters of the isotherms.

3.7.1. Langmuir isotherm

At room temperature (25 °C), Cr^{6+} ions adsorbed onto the DRA and CRA will be in equilibrium with Cr^{6+} ions in aqueous solution. The Langmuir isotherm model was chosen for the estimation of maximum sorption capacity corresponding to complete monolayer coverage on the sorbent surface. The saturated monolayer isotherm can be explained by the Langmuir non-linear equation as followed (Langmuir, 1916):

$$q_e = \frac{Q_m K_a C_e}{1 + K_a C_e} \quad (1)$$

where C_e is the equilibrium concentration (mg L^{-1}); q_e the amount of metal ion sorbed (mg g^{-1}); Q_m "maximum sorption capacity" is a complete monolayer (mg g^{-1}); K_a is sorption equilibrium constant (L mg^{-1}) that is related to the apparent energy of sorption. The Langmuir isotherm Eq. (1) can be linearized into four different forms (Eq. (2)), which give different parameter estimates (Longhinotti et al., 1998).

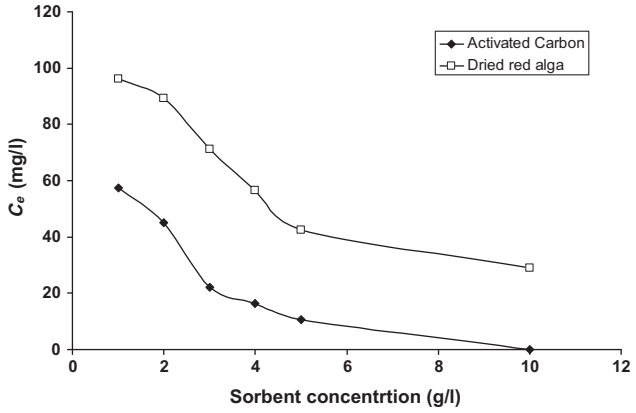

Figure 5 Effect of adsorbent concentration on Cr^{+6} removals (C_0: 125 mg L^{-1}, pH 1.0, agitation speed: 200 rpm, temperature: 25 °C).

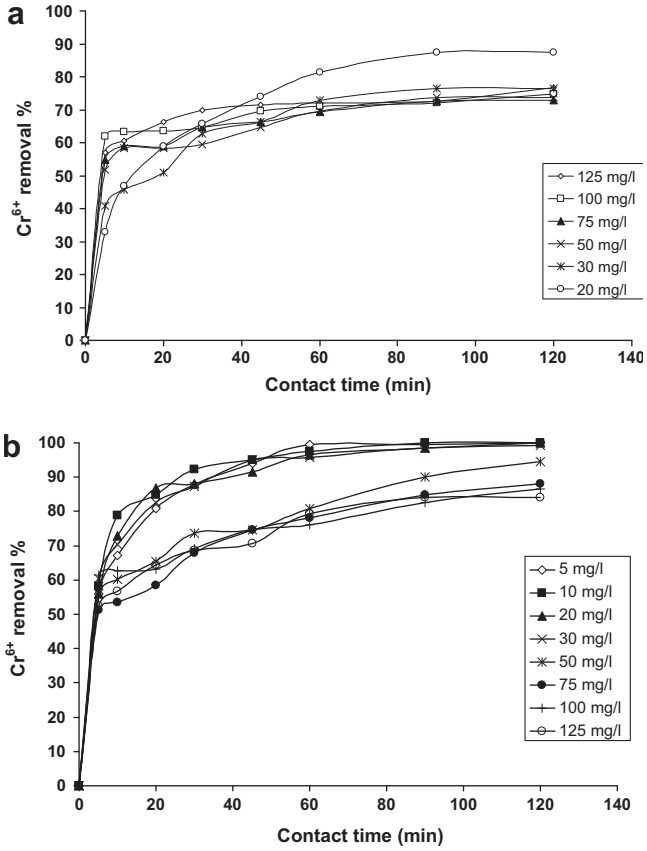

Figure 6 Effect of contact time on the removal of different initial concentrations of Cr^{6+} ions: (a) using DRA (10 g L^{-1}) at pH 1.0 and (b) using CRA (3 g L^{-1}) at pH 1.0.

$$\frac{C_e}{q_e} = \frac{1}{K_a Q_m} + \frac{1}{Q_m} \times C_e \tag{2}$$

The value of r^2 (correlation coefficient) shows that the sorption data for Cr^{6+} was fitted well into Langmuir sorption isotherm (Table 2) (Baran et al., 2005).

3.7.2. Freundlich isotherm

Freundlich model was chosen to estimate the sorption intensity of the sorbate on the sorbent surface. The empirical Freundlich isotherm, based on sorption heterogeneous surface, can be derived assuming a logarithmic decrease in the enthalpy of sorption with the increase in the fraction of occupied sites and is given by the following non-linear equation (Freundlich, 1906):

$$q_e = K_F C_e^{1/n} \tag{3}$$

where K_F and $1/n$ are the Freundlich constants characteristics of the system, indicating the sorption capacity and sorption intensity of metal ions on the sorbent, respectively. Eq. (3) can be linearized in logarithmic form Eq. (4) and the Freundlich constants can be determined.

$$\log q_e = \log K_F + \frac{1}{n} \log C_e \tag{4}$$

3.7.3. Redlich–Peterson isotherm

Redlich–Peterson isotherm (Redlich and Peterson, 1959) contains three parameters and involves the features of both Langmuir and Freundlich isotherms. It can be described in the following non-linear Eq. (4):

$$q_e = \frac{AC_e}{1 + BC_e^g} \tag{5}$$

It has three isotherm constants, namely, A, B and g, where g must fluctuate between zero and one and it can characterize the isotherm. If $g = 1$, Langmuir will be the preferable isotherm, while if $g = 0$, Freundlich will be the preferable isotherm. Eq. (5) can be converted to the next linear form through the logarithms as follows:

$$\ln\left(A\frac{C_e}{q_e} - 1\right) = g\ln(C_e) + \ln(B) \tag{6}$$

The isotherm constants can be evaluated from Eq. (5) using a trial-and-error optimization method, which is applicable to computer operation was developed to calculate the isotherm constants through maximization of the coefficient of determination and the results were included in Table 3.

3.7.4. Tempkin isotherm

Tempkin isotherm model was chosen to evaluate the sorption potentials of the sorbent for sorbates. The derivation of Tempkin isotherm assumes that the fall in the heat of sorption is linear rather than logarithmic, as implied in Freundlich equation. Tempkin isotherm has generally been applied in the following form Eq. (10) (Wang and Qin, 2005):

Table 2 Isotherm parameters obtained from the four linear forms of Langmuir model for the sorption of Cr^{6+} using dried red alga (DRA) and its activated carbon (CRA).

Langmuir	DRA concentration (g L^{-1})	CRA concentrations (g L^{-1})		
Wt.	10.0	3.0	4.0	5.0
Q_m	12.85	66.75	30.37	25.02
K_a	0.015	0.06	0.54	1.16
R^2	0.998	0.994	0.999	0.994

Q_m (mg g^{-1}) and K_a (L mg^{-1}).

Table 3 Comparison of the coefficients isotherm parameters for Cr^{6+} sorption by dried red alga (DRA) and its activated carbon (CRA).

Model	DRA concentration	CRA concentrations		
	10 (g L^{-1})	3 (g L^{-1})	4 (g L^{-1})	5 (g L^{-1})
Freundlich				
$1/n$	0.688	0.401	0.232	0.212
K_F (mg g^{-1})	0.752	10.32	14.26	14.08
R^2	0.913	0.996	1.000	1.000
Redlich–Peterson				
A (L g^{-1})	0.229	9.04	18.48	15.84
B (L $mg^{-1})^g$	0.023	0.43	0.61	0.26
g	0.739	0.767	1.00	1.00
R^2	0.958	0.989	0.982	1.000
Temkin				
A (L g^{-1})	0.461	2.71	12.30	30.49
b (mg L^{-1})	2.90	7.97	5.14	4.00
R^2	0.770	0.999	1.000	0.999
Dubinin–Radushkevich				
Q_m (mg g^{-1})	*11.77*	38.52	27.91	23.46
$K \times 10^6$ (mol^2 kJ^{-2})	*45.60*	8.10	0.70	0.20
E (kJ mol^{-1})	0.104	0.248	0.845	1.581
R^2	*0.966*	0.985	0.996	0.997

$$q_e = \frac{RT}{b} \ln (AC_e) \tag{7}$$

Eq. (6) can be simplified to the Eq. (7):

$$q_e = B \ln A + B \ln C_e \tag{8}$$

where $B = (RT)/b$, q_e (mg g^{-1}) and C_e (mg L^{-1}) are the amounts of adsorbed Cr^{6+} per unit weight of sorbent and unsorbed Cr^{6+} concentration in solution at equilibrium, respectively. Also, T is the absolute temperature in *Kelvin* and R is the universal gas constant, 8.314 J mol^{-1} K^{-1}. The constant b is related to the heat of sorption (Pearce et al., 2003; Akkaya and Ozer, 2005). The sorption data were analyzed according to the linear form of the Tempkin isotherm Eq. (7) and the results are shown in Table 3.

3.7.5. Dubinin–Radushkevich isotherm

Dubinin–Radushkevich (D–R) model was chosen to estimate the characteristic porosity and the apparent free energy of sorption (Radushkevich, 1949; Dubinin, 1960, 1965). The D–R isotherm is more general than the Langmuir isotherm, because it does not assume a homogeneous surface or constant sorption potential. The D–R model has generally been applied in the following form Eq. (8) and its linear form can be shown in Eq. (13):

$$q_e = Q_m \exp(-K\varepsilon^2) \tag{9}$$

$$\ln q_e = \ln Q_m - K\varepsilon^2 \tag{10}$$

where K is a constant related to the sorption energy, Q_m the theoretical saturation capacity, ε is the Polanyi potential, calculated from Eq. (10).

$$\varepsilon = RT \ln \left(1 + \frac{1}{C_e}\right) \tag{11}$$

The slope of the plot of $\ln q_e$ versus ε^2 gives K (mol^2 $(kJ^2)^{-1}$) and the intercept yields the sorption capacity, Q_m (mol g^{-1}). The mean free energy of sorption (E), defined as the free energy change when one mole of ion is transferred from infinity in solution to the surface of the solid, was calculated from the K value using the following relation Eq. (11) (Kundu and Gupta, 2006):

$$E = \frac{1}{\sqrt{2K}} \tag{12}$$

The calculated values of E are given in Table 3. The maximum sorption capacity obtained Q_m obtained using D–R isotherm model for sorption of Cr^{6+} over DRA was 11.77 mg g^{-1} (Table 3), which is very close to that obtained from Langmuir isotherm model (Table 2), while the Q_m obtained from D–R isotherm model for CRA (38.52 mg L^{-1}) is very far from that calculated from Langmuir isotherm model (Table 2). However, the Q_m calculated from D–R and Langmuir isotherm models at higher doses of activated carbon (4 and 5 g L^{-1}) were very close to each other. The typical range of bonding energy for ion-exchange mechanisms is 8–16 kJ mol^{-1}, while the values of E are 0.104 kJ mol^{-1} for DRA and 0.248, 0.845 and 1.581 kJ mol^{-1} for CRA, indicating that physisorption plays a significant role in the sorption process of Cr^{6+} ion onto DRA and CRA, which is in agreement with the result obtained from pH study for both DRA and CRA sorbents.

3.7.6. Choosing the best isotherm model

The results obtained in Table 2 showed the strong positive evidence that the sorption of chromium ions onto DRA and CRA follows the Langmuir isotherm. The applicability of the linear form of Langmuir model to both of two sorbents investigated was proved by the high correlation coefficients $R^2 > 0.994$. The Q_m obtained from the linear forms of Langmuir were ~12 and ~66 mg L^{-1} for DRA and CRA, respectively. The correlation coefficient obtained from Redlich–Peterson isotherm was higher than that obtained from Freundlich isotherm for data obtained from sorption of Cr^{6+} onto DRA, on the other hand, the sorption of Cr^{6+}

Table 4 Summary of some adsorbents used for the removal of Cr(VI) ions from aqueous solution.

Adsorbent	Q_{max} (mg g^{-1})	References
DRA	12.85	This work
CRA	66.67	This work
Terminalia arjuna nuts	28.43	Mohanty et al. (2005)
Chitosan	273	Udaybhaskar et al. (1990)
Non-crosslinked chitosan	80	Schmuhl et al. (2001)
Crosslinked chitosan	50	Schmuhl et al. (2001)
Commercial activated carbon (granular)	6.84	Monser and Adhoum (2002)
Fly ash–China clay	0.31	Panday et al. (1984)
Sphagnum peat moss	43.9	Sharma and Forster (1995)

over DRA is not modeled by Tempkin isotherm as well across the concentration range studied. This indicates that the sorption system is more likely monolayer coverage of DRA surface by the chromium ions.

The correlation coefficient obtained from analysis of the sorption of Cr^{6+} using activated carbon was high for all studied isotherm models, Langmuir, Freundlich Redlich–Peterson and Tempkin isotherm models, which indicates the presence of more than one sorption system in the case of using CRA as sorbent for chromium sorption. However, the four linear forms of Langmuir isotherm fit well the results for both the DRA and CRA for all the chromium ions concentration and sorbents doses, which indicate that the most-suitable isotherm for the data set was the Langmuir isotherm.

The different correlations of the various isotherm models applied for both DRA and CRA implies that different sorption mechanisms are involved for the alga and its activated carbon samples. The sorption capacities obtained for DRA and CRA are comparable to that obtained for some sorbents (Table 4) (Mohanty et al., 2005; Udaybhaskar et al., 1990; Schmuhl et al., 2001; Monser and Adhoum, 2002; Panday et al., 1984; Sharma and Forster, 1995) such as *Terminalia arjuna* nuts (Mohanty et al., 2005), Crosslinked chitosan (Schmuhl et al., 2001), commercial activated carbon (granular) and *Sphagnum* peat moss (Sharma and Forster, 1995) and much more than that reported for Fly ash–China clay (Panday et al., 1984).

3.8. Kinetic studies

The kinetics of sorption describes the rate of chromium ions uptake on DRA and CRA and this rat controls the equilibrium time. The kinetics of Cr^{6+} sorption DRA and CRA is required for selecting optimum operating conditions for the full-scale batch process. The kinetic parameters, which are helpful for the prediction of sorption rate, give important information for designing and modeling the processes. Thus, the kinetics of Cr^{6+} sorption on the activated carbons were analyzed using pseudo first-order (Lagergren, 1898), pseudo second-order (Ho et al., 2000), Elovich (Zeldowitsch, 1934; Chien and Clayton, 1980; Sparks 1986) and intraparticle diffusion (Weber and Morris, 1963; Srinivasan et al., 1988) kinetic models. The conformity between experimental data and the model-predicted values were expressed by the correlation coefficients (R^2, values close or equal to 1). The relatively higher value is the more applicable model to the kinetics of Cr^{6+} sorption.

3.8.1. Pseudo first-order kinetic model

The kinetic data were treated with the Lagergren first-order model (Lagergren, 1898), which is the earliest known one describing the sorption rate based on the sorption capacity. It is generally expressed as follows:

$$\frac{dq_t}{dt} = k_1(q_e - q_t) \tag{13}$$

where, q_e and q_t are the sorption capacities at equilibrium and at time t, respectively (mg g^{-1}), k_1 is the rate constant of pseudo first-order sorption (L min^{-1}). Eq. (12) was integrated with the boundary conditions of $t = 0$ to $t = t$ and $q_t = 0$ to $q_t = q_t$ and rearranged to the following linear equation:

$$\log(q_e - q_t) = \log(q_e) - \frac{k_1}{2.303}t \tag{14}$$

The values of log $(q_e - q_t)$ were linearly correlated with t. The plot of log $(q_e - q_t)$ versus t should give a linear relationship from which k_1 and predicted q_e can be determined from the slope and intercept of the plot, respectively. The variation in rate should be proportional to the first power of concentration for strict surface sorption. However, the relationship between initial solute concentration and rate of sorption will not be linear when pore diffusion limits the sorption process. It was observed that the Lagergren model fits well for the first 20 min and thereafter the data deviate from theory. Thus, the model represents the initial stages where rapid sorption occurs well but cannot be applied for the entire sorption process. On the other hand, the experimental q_e values do not agree with the calculated ones, obtained from the linear plots even the correlation coefficient R^2 is relatively high (Table 5). This shows that the sorption of Cr^{6+} onto DRA and CRA can be applied but not appropriate to describe the entire process which is not a first-order reaction.

3.8.2. Pseudo second-order kinetic model

Sorption kinetic was explained by the pseudo-second-order model given by Ho and McKay (Ho et al., 2000) as follows:

$$\frac{dq_t}{dt} = k_2(q_e - q_t)^2 \tag{15}$$

where k_2 (g mg^{-1} min^{-1}) is the second-order rate constant of sorption. Integrating Eq. (18) for the boundary conditions $q = 0$ to $q = q_t$ at $t = 0$ to $t = t$ is simplified as can be rearranged and linearized to obtain:

$$\left(\frac{t}{q_t}\right) = \frac{1}{k_2 q_e^2} + \frac{1}{q_e}(t) \tag{16}$$

Table 5 Comparison of the first- and second-order sorption rate constants, calculated and experimental q_e values for sorption of Cr^{6+} with different initial concentrations onto dried red alga (DRA) and its activated carbon (CRA) concentrations.

Parameter		First-order kinetic model				Second-order kinetic model			
Sorbent Concentration	C_0 of Cr concentration	q_e (exp.)	k_1	q_e (calc.)	R^2	k_2	q_e (calc.)	h	R^2
DRA									
10 (g L^{-1})	20	1.75	0.04	1.20	0.992	0.044	1.93	0.16	0.998
	50	3.68	0.03	1.31	0.955	0.049	3.82	0.72	0.997
	75	5.47	0.03	1.51	0.982	0.044	5.63	1.40	0.999
	100	7.47	0.02	1.49	0.952	0.042	7.55	2.42	0.999
	125	9.60	0.03	2.49	0.942	0.033	9.64	3.11	0.999
CRA									
3 (g L^{-1})	20	6.67	0.04	2.63	0.966	0.032	6.90	1.50	1.000
	50	15.74	0.02	6.81	0.965	0.007	16.42	1.85	0.992
	75	22.04	0.03	11.82	0.987	0.009	19.34	3.54	0.998
	100	28.86	0.02	10.53	0.968	0.006	27.93	4.85	0.994
	125	34.99	0.02	8.27	0.946	0.006	35.23	8.98	0.998
4 (g L^{-1})	20	5.00	0.05	2.30	0.974	0.043	5.21	1.16	1.000
	50	12.50	0.02	6.16	0.980	0.008	13.02	1.36	0.993
	75	18.06	0.03	9.50	0.965	0.006	18.94	2.10	0.993
	100	23.85	0.02	10.27	0.974	0.005	24.75	3.28	0.994
	125	27.20	0.02	7.96	0.954	0.008	27.93	6.02	0.998
5 (g L^{-1})	20	4.00	0.07	1.28	0.989	0.140	4.07	2.31	1.000
	50	10.00	0.03	5.10	0.992	0.013	10.59	1.44	0.998
	75	14.75	0.04	7.95	0.967	0.009	15.63	2.18	0.996
	100	19.57	0.03	7.89	0.995	0.008	20.37	3.19	0.997
	125	22.97	0.02	6.00	0.955	0.009	23.53	5.25	0.997

C_0 (mg L^{-1}), q_e (mg g^{-1}), k_1 (min^{-1}), k_2 (g mg^{-1} min^{-1}) and h (mg g^{-1} min^{-1}).

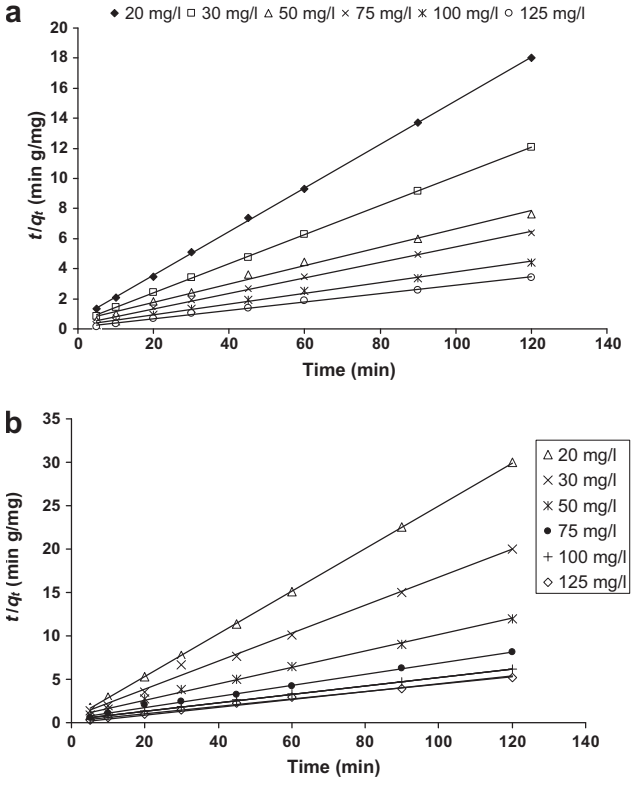

Figure 7 Plot of the pseudo-second-order model at different initial Cr^{6+} concentrations: (a) DRA 10 g L^{-1}, pH 1, temperature 25 °C and (b) CRA 10 g L^{-1}, pH 1, temperature 25 °C.

The second-order rate constants were used to calculate the initial sorption rate, given by the following Eq. (16):

$$h = k_2 q_e^2 \tag{17}$$

If the second-order kinetics is applicable, then the plot of t/q_t versus t should show a linear relationship. Values of k_2 and equilibrium sorption capacity q_e were calculated from the intercept and slope of the plots of t/q_t versus t (Fig. 7). The linear plots of t/q_t versus t show good agreement between experimental and calculated q_e values at different initial Cr^{6+} and adsorbent concentrations (Table 5). The correlation coefficients for the second-order kinetic model are greater than 0.990. In the view of these results, it is believed that the pseudo-second-order kinetic model provided good correlation for the sorption of Cr^{6+} onto DRA and CRA at different initial Cr^{6+} and sorbent concentrations in contrast to the pseudo-first-order model and intraparticle diffusion model.

Moreover, values for the product h (initial sorption) that represents the rate of initial sorption, is practically increased from 0.16 to 3.11 and 1.50 to 8.98, 1.16 to 6.02 and 1.44 to 5.25 mg g^{-1} min^{-1} with the increase in initial Cr^{6+} concentrations from 20 to 125 mg L^{-1} using dried red alga (10 g L^{-1}) and its activated carbon (3, 4 and 5 g L^{-1}), respectively. Also, initial sorption rate decreased from 8.98 to 5.25 mg g^{-1} min with the increase in activated carbon dose concentrations from 3 to 5 g L^{-1} for 125 mg L^{-1} of Cr^{6+} concentration (Table 5). It was observed that the pseudo-second-order rate constant (k_2) decreased with the increase in initial Cr^{6+} concentration for all studied doses of DRA and CRA.

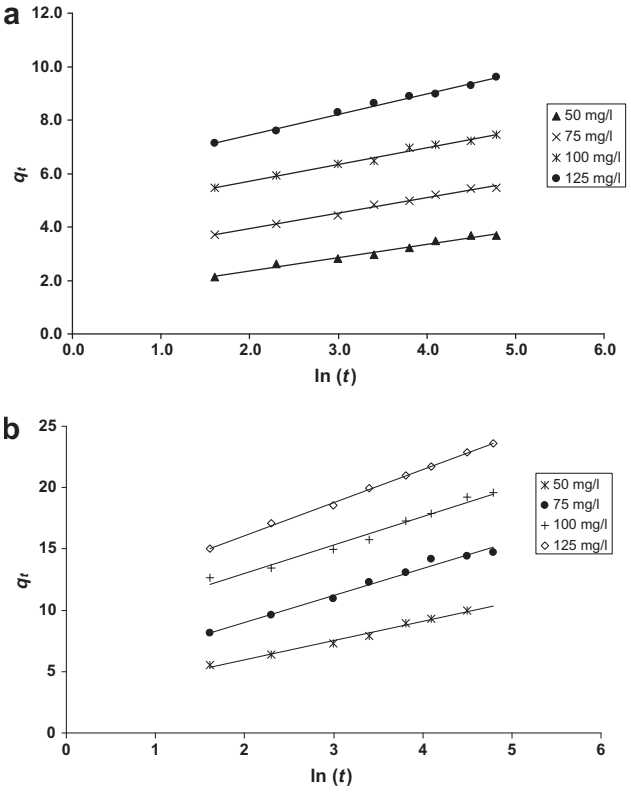

Figure 8 Elovich model plot for the sorption of Cr^{6+} onto: (a) DRA (10 g L^{-1}) and (b) CRA (5 g L^{-1}) at different initial chromium concentrations (50, 75, 100 and 125 mg L^{-1}).

3.8.3. Elovich kinetic model

Elovich kinetic equation is another rate equation based on the sorption capacity, which is generally expressed as (Zeldowitsch, 1934; Chien and Clayton, 1980; Sparks, 1986):

$$\frac{dq_t}{dt} = \alpha \exp(-\beta q_t) \tag{18}$$

where α is the initial sorption rate (mg g^{-1} min^{-1}) and β is the de-sorption constant (g mg^{-1}) during any one experiment.It is simplified by assuming $\alpha\beta t \gg t$ and by applying the boundary conditions $q_t = 0$ at $t = 0$ and $q = q_t$ at $t = t$ Eq. (18) is formed as follows:

$$q_t = \frac{1}{\beta}\ln(\alpha\beta) + \frac{1}{\beta}\ln(t) \tag{19}$$

If Cr^{6+} sorption by DRA and CRA fits the Elovich model, a plot of q_t versus ln (t) should yield a linear relationship with a slope of $(1/\beta)$ and an intercept of $(1/\beta) \times \ln(\alpha\beta)$ (Fig. 8). Thus, the constants can be obtained from the slope and the intercept of the straight line (Table 6). For DRA, the initial sorption rate α increase from 7.84 to 1650.81 mg g^{-1} min^{-1} with the increase of the initial chromium concentration from 50 to 125 mg g^{-1}, while α increase from 29.09 to 280.87, 8.28 to 199.99 and 9.42 to 144.29 mg g^{-1} min with increase of initial chromium concentration from 50 to 125 mg L^{-1} if adsorbed onto 3, 4 and 5 g L^{-1} of CRA, respectively. Similar pattern is mentioned above for the initial sorption rate, h, obtained from pseudo-second-order model. The desorption constant, β, decrease from 2.01 to 1.3 g mg^{-1} with the increase of initial chromium concentration from 50 to 125 mg L^{-1}, while β decrease from 0.49 to 0.25, 0.50 to 0.33 and 0.64 to 0.37 g mg^{-1} with the same increase in the initial chromium concentration over CRA of 3, 4 and 5 g L^{-1} (Table 6).

3.8.4. The intraparticle diffusion model

The intraparticle diffusion kinetic model can be applicable if the rate limiting step is the diffusion of metal ions into the sorbents (Weber and Morris, 1963; Srinivasan et al., 1988). The possibility of intra-particular diffusion is explored by using the following equation:

$$q_t = K_{dif}t^{1/2} + C \tag{20}$$

Table 6 The parameters obtained from Elovich kinetics model and intraparticle diffusion model using different initial chromium concentrations.

Sorbent dose	(C_0) Cr^{6+}	Elovich			Intraparticle diffusion		
		β	α	R^2	K_{dif}	C	R^2
DRA							
10 (g L^{-1})	50	2.01	7.84	0.981	0.19	1.91	0.991
	75	1.72	67.91	0.990	0.23	3.41	0.971
	100	1.59	760.63	0.989	0.15	5.82	0.979
	125	1.30	1650.8	0.992	0.17	7.82	0.979
CRA							
3 (g L^{-1})	50	0.49	29.09	0.948	0.79	7.31	0.981
	75	0.32	24.78	0.953	0.98	13.22	0.990
	100	0.25	39.57	0.996	0.98	18.11	0.986
	125	0.25	280.87	0.989	0.76	27.11	0.976
4 (g L^{-1})	50	0.51	8.28	0.991	0.60	5.98	1.000
	75	0.35	12.17	0.993	0.79	9.54	0.983
	100	0.28	21.67	0.998	0.86	14.57	0.963
	125	0.33	199.99	0.992	0.71	19.61	0.956
5 (g L^{-1})	50	0.64	9.42	0.989	0.26	7.27	0.960
	75	0.46	18.41	0.985	0.15	13.03	0.957
	100	0.43	84.29	0.980	0.57	13.48	0.960
	125	0.37	144.23	0.999	0.32	18.29	0.993

C_0 (mg L^{-1}), α (g mg^{-1}), β (mg g^{-1} m^{-1}), K_{dif} (mg g^{-1} $min^{-1/2}$) and C (mg g^{-1}).

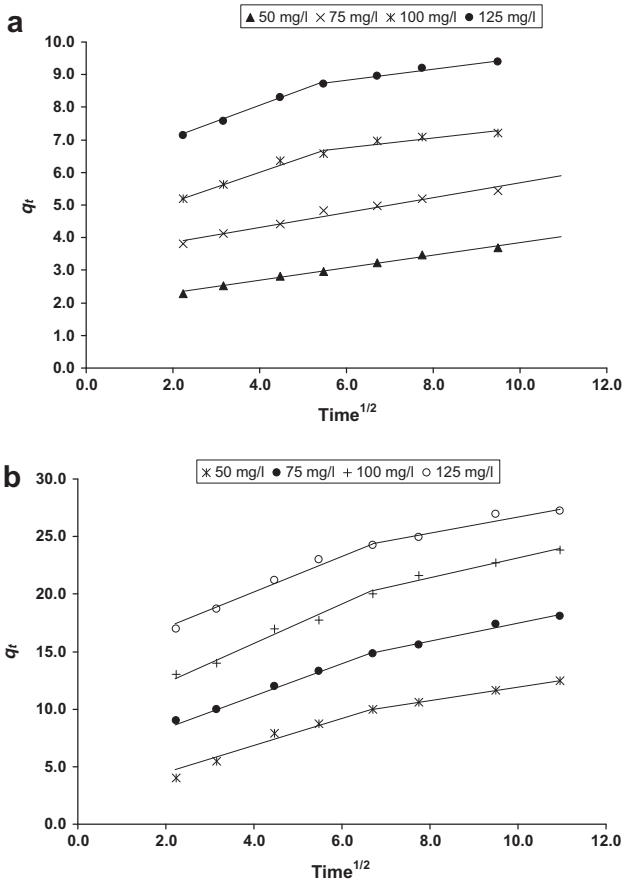

Figure 9 Intraparticle diffusion model plot for the sorption of Cr^{6+} onto: (a) DRA (10 g L^{-1}) and (b) CRA (4 g L^{-1}) at different initial chromium concentrations (50, 75, 100 and 125 mg L^{-1}).

where C is the intercept and K_{dif} is the intra-particle diffusion rate constant. The values of q_t correlated linearly with values of $t^{1/2}$ (Fig. 9) and the rate constant K_{dif} directly evaluated from the slope of the regression line.

The values of intercept C (Table 6) provide information about the thickness of the boundary layer, the resistance to the external mass transfer increase as the intercept increase. R^2 values given in Table 6 are more than 0.95 for both sorbents used in this study, confirming that the rate-limiting step is actually the intra-particle diffusion process. The intra-particle diffusion rate constant, K_{dif}, was in the range of (0.15–0.23 mg g^{-1} $min^{-0.5}$) and (0.15–0.98 mg g^{-1} $min^{-0.5}$) for DRA and CRA, respectively. The linearity of the plots demonstrated that intra-particle diffusion played a significant role in the uptake of the chromium by sorbent. However, Fig. 9a shows two lines at high initial chromium concentrations over DRA, while Fig. 9b shows two lines for all studied initial chromium concentrations over activated carbon, which confirms that sorption of the chromium onto the DRA and its activated carbon is independent of one another, as plot usually shows two or more intersecting lines depending on the exact mechanism, the first one of these lines representing surface sorption and the second one intra-particle diffusion. The absence of such features in the plots of DRA at initial chromium concentrations of 50 and 75 mg L^{-1} indicated that the steps were indistinguishable from one another and that the intraparticle diffusion is the prominent process right from the beginning of chromium–DRA interaction. However, still there is no sufficient indication about which of the two steps was the rate-limiting step. Ho (2003) has shown that if the intraparticle

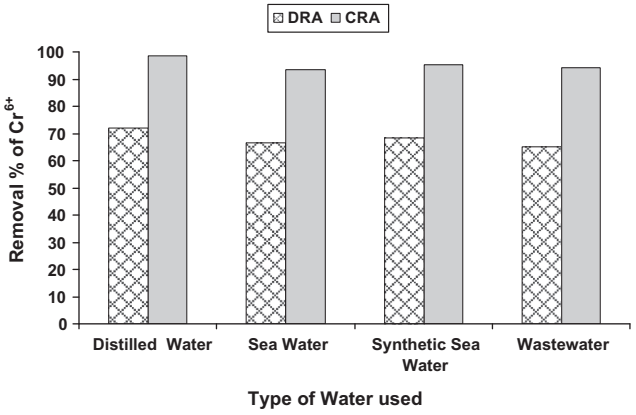

Figure 10 Effect of saline water and wastewater on the removal of chromium using dried red alga (DRA) and its activated carbon (CRA).

diffusion is the sole rate-limiting step, it is essential for the q_t versus $t^{1/2}$ plots to pass through the origin, which is not the case in both of Fig. 9, it may be concluded that surface sorption and intraparticle diffusion were concurrently operating during the chromium–DRA and CRA interactions. Therefore, the intraparticle diffusivity is the slower step in the sorption process and its effect on CRA is smaller due to porosity of the material. Meanwhile, at low initial concentrations of Cr, the dual mechanism is not so obvious in the case of DRA, which may be attributed to the fact that the majority of the sorbed quantity is in the outer surface of the material.

3.9. Applicability

With the above results in hand, our attention was turned toward the study of the effect of salinity and real wastewater on the capability of the DRA and CRA on removal of Cr^{6+} ions from solution. The above work was achieved using synthetic sea water, natural sea water and real wastewater. Fig. 10 shows that the percentage of Cr^{6+} removal from aqueous solution prepared by dissolving of the Cr^{6+} into distilled water, wastewater, sea water and synthetic sea water was near 65% and 94% for DRA and CRA, respectively, which indicates that the maximum sorption capacities were not affected by the changing of the type of chromium solution. These results indicate that the two sorbents DRA and CRA are applicable material for removal of Cr^{6+} ions from different types of aqueous solutions including wastewater.

4. Conclusion

The indigenous DRA and CRA have been identified as effective adsorbents to remove different initial concentrations of toxic Cr^{6+} ions from various types of its aqueous solutions. The sorption process is related to the pH of solution, pH 1.0 is the optimal. The sorption kinetic data can be described by the second-order kinetic and Elovich models. Furthermore, the equilibrium data of sorption are in good agreement with the four linear forms of Langmuir model. The CRA exhibited high sorption capacity under several initial chromium and sorbent dose concentrations. The sorption process was found to be controlled by the film diffusion at lower concentrations of the sorbate and shifted to particle diffusion at high concentration. The proposed sorbents are efficient, environment friendly and can reduce the huge amount of indiscriminate effluent discharges around the small industry concerns.

References

Abdelwahab, O., El Nemr, A., El-Sikaily, A., Khaled, A., 2006a. Chem. Ecol. 22, 253.

Abdelwahab, O., El-Sikaily, A., El Nemr, A., Khaled, A., 2006b. In: International Conference on Aquatic Resources: Needs and Benefits NIOF, 18–21st September 2006, Alexandria, Egypt, p. 54.

Abdelwahab, O., El Sikaily, A., Khaled, A., El Nemr, A., 2007. Chem. Ecol. 23 (1), 73.

Ahalya, N., Kanamadi, R.D., Ramachandra, T.V., 2005. Electron. J. Biotechnol. 8 (3), 258.

Akkaya, G., Ozer, A., 2005. Process Biochem. 40 (11), 3559.

Babel, S., Kurniawan, T.A., 2003. J. Hazard. Mater. B97, 219.

Baran, A., Baysal, S.H., Sukatar, A., 2005. J. Environ. Biol. 26, 329.

Cesar Ricardo, T.T., Marco Aurelio, Z.A., 2004. Chemosphere 54, 987.

Chandra, N., Agnihotri, N., Sharma, P., Bhasin, S., Amritphale, S.S., 2005. J. Sci. Ind. Res. 64, 674.

Chien, S.H., Clayton, W.R., 1980. Soil Sci. Soc. Am. J. 44, 265.

Davis, T.A., Volesky, B., Mucci, A., 2003. Water Res. 37, 4311.

Demirbas, E., Kobya, M., Senturk, E., Ozkan, T., 2004. Water SA 30 (40), 533.

Deng, L., Zhang, Y., Qin, J., Wang, X., Zhu, X., 2009. Miner. Eng. 22 (4), 372.

Dubinin, M.M., 1960. Chem. Rev. 60, 235.

Dubinin, M.M., 1965. Zhurnal Fizicheskoi Khimii 39, 1305.

El Nemr, A., El-Sikaily, A., Khaled, A., Abdelwahab, O., 2006. Abstract. In: International Conference on Aquatic Resources: Needs and Benefits NIOF, 18–21st September, Alexandria, Egypt, p. 58.

El Nemr, A., El-Sikaily, A., Khaled, A., 2010. Egypt. J. Aquat. Res. 36 (3), 403.

El Nemr, A., Khaled, A., El Sikaily, A., Abdelwahab, O., 2007. Chem. Ecol. 23 (2), 119.

El-Sikaily, A., Khaled, A., El-Nemr, A., Abdelwahab, O., 2006. Chem. Ecol. 22, 149.

Freundlich, H.M.F., 1906. Zeitschrift für Physikalische. Chemie (Leipzig) 57 (A), 385.

Gilcreas, F.W., Tarars, M.J., Ingols, R.S., 1965. Standard Methods for the Examination of Water and Wastewater, 12th ed. American Public Health Association (APHA) Inc., New York, 1965, p. 213.

Gode, F., Pehlivan, E., 2005. J. Hazard. Mater. B, 119–175.

Griffen, G., 1971. Interpretation of X-ray diffraction data. In: Carver, R.E. (Ed.), Procedures in Sedimentary Petrology. Wiley Interscience, New York, p. 41.

Gupta, V.K., Rastogi, A., 2009. J. Hazard. Mater. 163 (1), 396.

Gupta, V.K., Shrivastava, A.K., Jain, N., 2001. Water Res. 35 (17), 4079.

Han, X., Wong, Y.S., Wong, M.H., Tam, N.F.Y., 2008. J. Hazard. Mater. 158 (2-3), 615.

Hawari, A.H., Mulligan, C.N., 2006. Process Biochem. 41, 187.

Ho, Y.S., 2003. Water Res. 37, 2323.

Ho, Y.S., McKay, G., Wase, D.A.J., Foster, C.F., 2000. Sci. Technol. 18, 639.

Kalyani, S., Srinivasa Roa, P., Krishnaiah, A., 2004. Chemosphere 57, 1225.

Kamath, S.R., Proctor, A., 1998. Chemosphere 75, 484.

Ko, Y.G., Choi, U.S., Kim, T.Y., Ahn, D.J., Chn, Y.J., 2002. Rapid Commun. 23, 535.

Kundu, S., Gupta, A.K., 2006. Colloids Surf., A: Physicochem. Eng. Aspects 273, 121.

Lagergren, S., 1898. Kungliga Svenska Vetenskapsakademiens. Handlingar 24, 1.

Langmuir, I., 1916. J. Am. Chem. Soc. 38, 2221.

Longhinotti, E., Pozza, F., Furlan, L., Sanchez, M.D.N.D., Klug, M., Laranjeira, M.C.M., Favere, V.T., 1998. J. Braz. Chem. Soc. 9, 435.

Malkoç, E., Nuhoglu, Y., 2003. Fresenius Environ. Bull. 12 (4), 376.

Malkoc, E., Nuhoglu, Y., 2006. J. Hazard. Mater. 135 (1-3), 328.

McKay, G., Ho, Y.S., Ng, J.C.Y., 1999. Sep. Purif. Methods 28, 87.

Meena, A.K., Mishra, G.K., Kumar, S., Rajagopal, C., Nagar, P.N., 2004. J. Sci. Ind. Res. 63, 410.

Mohanty, K., Jha, M., Eikap, M B.C., Biswas, M.N., 2005. Chem. Eng. Sci. 60, 3049.

Monser, L., Adhoum, N., 2002. Sep. Purif. Technol. 26, 137.

Ncibi, M.C., Ben Hamissa, A.M., Fathallah, A., Kortas, M.H., Baklouti, T., Mahjoub, B., Seffen, M., 2009. J. Hazard. Mater. 170 (2-3), 1050.

Padilha, F.P., PessôedeFranca, F., Augustodacosta, A.C., 2005. Bioresour. Technol. 96 (13), 1511.

Panday, K.K., Prasad, G., Singh, V.N., 1984. J. Chem. Technol. Biotechnol. 34A, 367.
Pearce, C.I., Lioyd, J.R., Guthrie, J.T., 2003. Dyes Pigm. 58, 179.
Pellerin, C., Booker, S.M., 2000. Environ. Health Perspect. 108 (9), 402.
Radushkevich, L.V., 1949. Zhurnal Fizicheskoi Khimii 23, 1410.
Ramos, R.L., Martinez, A.J., Coronado, R.M.G., 1994. Water Sci. Technol. 30 (9), 191.
Redlich, O., Peterson, D.L., 1959. J. Phys. Chem. 63, 1024.
Richard, F.C., Bourg, A.C.M., 1991. Water Res. 25 (7), 807.
Schmuhl, R., Krieg, H.M., Keizer, K., 2001. Water SA 27 (1), 1.
Sharma, D.C., Forster, C.F., 1995. Process Biochem. 30 (4), 293.
Sparks, D.L., 1986. Kinetics of Reaction in Pure and Mixed Systems, in Soil Physical Chemistry. CRC Press, Boca Raton.
Srinivasan, K., Balasubramanian, N., Ramakrishan, T.V., 1988. Ind. J. Environ. Health 30, 376.
Udaybhaskar, P., Iyengar, L., Rao, A.V.S.P., 1990. J. Appl. Polym. Sci. 39, 739.
Vieira, R.H.S.F., Volesky, B., 2000. Int. Microbiol. 3, 17.
Vijayaraghavan, K., Jegan, J., Palanivelu, K., Velan, M., 2005. Chem. Eng. J. 106, 177.
Villaescusa, I., Fiol, N., Martinez, M., Miralles, N., Poch, J., Serarols, J., 2004. Water Res. 38, 992.
Wang, X.S., Qin, Y., 2005. Process Biochem. 40, 677.
Wang, X.S., Tang, Y.P., Tao, S.R., 2009. Chem. Eng. J. 148 (2-3), 217.
Weber, W.J., Morris, J.C., 1963. J. Sanit. Eng. Div. Am. Soc. Civ. Eng. 89, 31.
Zakhama, S., Dhaouadi, H., M'Henni, F., 2011. Bioresour. Technol. 102 (2), 786.
Zeldowitsch, J., 1934. Acta Phys. Chim. URSS 1, 364.
Zeroual, Y., Moutaouakkil, A., Dzairi, F.Z., Talbi, M., Chung, P.U., Lee, K., Blaghen, M., 2003. Bioresour. Technol. 90, 349.